

Single-cell RNA landscape of the special fiber initiation process in *Bombax ceiba*

Yuanhao Ding^{1,2,6}, Wei Gao^{4,6}, Yuan Qin^{5,6}, Xinping Li^{1,6}, Zhennan Zhang⁴, Wenjie Lai¹, Yong Yang¹, Kai Guo³, Ping Li¹, Shihan Zhou¹ and Haiyan Hu^{1,2,*}

¹Hainan Key Laboratory for Sustainable Utilization of Tropical Bioresources, College of Tropical Crops, Hainan University, Haikou 570228, China

²Sanya Nanfan Research Institute of Hainan University, Hainan Yazhou Bay Seed Laboratory, Sanya 572000, China

³College of Agronomy and Biotechnology, Southwest University, Chongqing 400716, China

⁴State Key Laboratory of Cotton Biology, School of Life Science, Henan University, Kaifeng, Henan, P.R. China

⁵MARA Key Laboratory of Sustainable Crop Production in the Middle Reaches of the Yangtze River (Co-construction by Ministry and Province), College of Agriculture, Yangtze University, Jingzhou 434025, China

⁶These authors contributed equally to this article.

*Correspondence: Haiyan Hu (huhaiyan@hainanu.edu.cn)

<https://doi.org/10.1016/j.xplc.2023.100554>

ABSTRACT

As a new source of natural fibers, the *Bombax ceiba* tree can provide thin, light, extremely soft and warm fiber material for the textile industry. Natural fibers are an ideal model system for studying cell growth and differentiation, but the molecular mechanisms that regulate fiber initiation are not fully understood. In *B. ceiba*, we found that fiber cells differentiate from the epidermis of the inner ovary wall. Each initiated cell then divides into a cluster of fiber cells that eventually develop into mature fibers, a process very different from the classical fiber initiation process of cotton. We used high-throughput single-cell RNA sequencing (scRNA-seq) to examine the special characteristics of fiber initiation in *B. ceiba*. A total of 15 567 high-quality cells were identified from the inner wall of the *B. ceiba* ovary, and 347 potential marker genes for fiber initiation cell types were identified. Two major cell types, initiated fiber cells and epidermal cells, were identified and verified by RNA *in situ* hybridization. A developmental trajectory analysis was used to reconstruct the process of fiber cell differentiation in *B. ceiba*. Comparative analysis of scRNA-seq data from *B. ceiba* and cotton (*Gossypium hirsutum*) confirmed that the additional cell division process in *B. ceiba* is a novel species-specific mechanism for fiber cell development. Candidate genes and key regulators that may contribute to fiber cell differentiation and division in *B. ceiba* were identified. This work reveals gene expression signatures during *B. ceiba* fiber initiation at a single-cell resolution, providing a new strategy and viewpoint for investigation of natural fiber cell differentiation and development.

Key words: *Bombax ceiba*, fiber initiation, single-cell RNA-seq

Ding Y., Gao W., Qin Y., Li X., Zhang Z., Lai W., Yang Y., Guo K., Li P., Zhou S., and Hu H. (2023). Single-cell RNA landscape of the special fiber initiation process in *Bombax ceiba*. Plant Comm. 4, 100554.

INTRODUCTION

Bombax ceiba L., commonly known as the red silk cotton tree, is a tall, deciduous, diploid tree with a height up to 40 m. *B. ceiba* is widely distributed in tropical and subtropical regions and is an important component of the tropical dry deciduous forest ecosystem (Trapnell et al., 2014). *B. ceiba* is a multipurpose tree species of tropical forests with medicinal, economic, and ecological benefits (Sharma et al., 2020). The fiber from mature *B. ceiba* fruits is a new natural fiber source for the textile industry because it is extremely thin, light, and soft (Rijavec, 2008). *B. ceiba* fibers also have many special features that give them a wide range of uses: they are bright, antibacterial,

moth-proof, mildew-proof, difficult to entangle, warm, hygroscopic, impervious to water, and not conductive of heat (Sunmonu and Abdullahi, 1992). The physical properties of *B. ceiba* fibers are well studied, but the biological processes that underlie their development remain to be clarified.

Both *B. ceiba* and cotton (*Gossypium hirsutum*) produce single-cell fibers, and both are species from the Malvaceae family, which

Published by the Plant Communications Shanghai Editorial Office in association with Cell Press, an imprint of Elsevier Inc., on behalf of CSPB and CEMPS, CAS.

suggests that their molecular mechanisms of fiber development are likely to be similar. Cotton fibers are the trichomes of the seed and develop from the outer epidermis of the ovule (Haigler et al., 2012). Previous studies have shown that the molecular mechanisms of fiber development in cotton may be similar to those of trichome development in *Arabidopsis* (Wang et al., 2013). The R2R3-MYB/bHLH/WD40 (MBW) complex of GL1 (GLABROUS1), TTG1 (TRANSPARENT TESTA GLABRA1), and GL3 (GLABRA 3) or EGL3 (ENHANCER OF GLABRA3) transcription factors (TFs) regulates GL2 (GLABRA 2), a downstream TF that is involved in trichome initiation in *Arabidopsis* (Ishida et al., 2008). Cotton homologs of these genes, such as *GaMYB2* (homolog of *AtGL1*), *GaHOX1* (homolog of *AtGL2*), *GhDEL65* (homolog of *AtGL3*), and *GhTTG1* and *GhTTG3* (homologs of *AtTTG1*), can often rescue the phenotypes of homologous gene mutants in *Arabidopsis* and function in regulating cotton fiber initiation (Wang et al., 2004; Humphries et al., 2005; Guan et al., 2008; Shangguan et al., 2016). Interestingly, researchers have found that several important TFs have species-specific roles in cotton fiber initiation; these include *GhMYB25*, *GhMYB25-like*, *PROTODERMAL FACTOR1* (*GhPDF1*), class-IV HD-ZIP factor (*GhHD1*), and *Gh14-3-3* (Machado et al., 2009; Walford et al., 2011, 2012; Deng et al., 2012; Zhou et al., 2015). Various hormone signals have also been shown to participate in cotton fiber initiation (Hu et al., 2016; Zhang et al., 2017; Zeng et al., 2019). Despite these findings, we lack a unified theory for fiber initiation. The natural fibers of *B. ceiba* are unusual in that they differentiate from the inner ovary wall, but the fiber initiation process in *B. ceiba* has received little attention.

The complexity of plant cells at the single-cell level has long been an active area of interest in plant biology (Ziegenhain et al., 2017). The application of single-cell RNA sequencing (scRNA-seq) methods has provided new insights into the heterogeneity of gene expression in different cells, the dynamics of cell types during development, and the expression characteristics of rare cell types (Wagner et al., 2016; Hwang et al., 2018). scRNA-seq has been widely used in model and nonmodel plants and yields complete cell-type-specific information for different tissues (Zhang et al., 2019; Liu et al., 2021). scRNA-seq can reveal the gene expression of cells throughout their differentiation (Liu et al., 2020). For example, the developmental trajectories from meristematic mother cells to guard mother cells in the stomatal lineage were analyzed by scRNA-seq in *Arabidopsis* (Liu et al., 2020). scRNA-seq of rice (*Oryza sativa*) roots was used to reconstruct the optimal developmental trajectory of epidermal cells and ground tissues, revealing conserved and differentiated root developmental pathways between dicots and monocots (Zhang et al., 2021). As a classical single-cell differentiation phenomenon, fiber initiation is a dynamic process that involves the transformation of epidermal cells into fiber cells. scRNA-seq offers researchers a chance to investigate changes in gene expression during fiber initiation at the single-cell level.

Fiber initiation serves as an ideal model system for studying cell growth and differentiation (Yang and Ye, 2013). *B. ceiba* fibers are single-cell fibers that develop from the epidermis of the inner ovary wall. The number of fiber initiation cells is one of the important factors that determine fiber yield. In this study, protoplasts isolated from inner ovary wall cells of *B. ceiba* were used to select a suitable cell population for scRNA-seq to clarify the key devel-

opmental processes and expressed genes involved in *B. ceiba* fiber initiation. The study of *B. ceiba* fiber initiation provides insights into plant cell fate specification and generates new gene resources for improving fiber yield and quality, especially in cotton.

RESULTS

Identification of fiber initiation and protoplast isolation from *B. ceiba*

To confirm the timing of fiber initiation in *B. ceiba*, a large number of flowers and capsules were collected and observed at different days post-anthesis (DPA), and the developmental statuses of the ovaries and fibers were recorded (Figure 1A–1L). The results showed that the buds undergo a long period of vegetative growth before flowering (Figure 1A). At –3 DPA, the flower buds enter a rapid growth stage, and the petals clearly begin to elongate (Figure 1B). At –1 DPA, the flower buds have elongated and swelled to their maximum size (Figure 1C). The flower then blooms at midnight and remains open until the next morning (0 DPA, flowering day), with the petals curling outward (Figure 1D). The flower remains in full bloom for 2–4 days, after which time the petals gradually retract and fade, and the ovary begins to expand. The diameter and length of the fertilized capsule increase dramatically over time (Figure 1D–1L). After capsules have matured, soft fibers are shed from the inner wall and tightly surround the seeds, waiting for the wind to carry them far from the parent plant (Supplemental Figure 1). Our measurements indicated that the length of mature *B. ceiba* fibers ranges from 21 to 26 mm, and no fuzz fibers were found (Supplemental Figure 2A).

From 8 to 11 DPA, some epidermal cells of the inner ovary wall begin to differentiate into fiber cells (Supplemental Figure 2B). The number of initiated fiber cells continues to increase as the capsules develop. Scanning electron microscopy revealed that some epidermal cells of the inner ovary wall had completed the initiation process, including fiber cell differentiation and division, by 11 DPA (Figure 1M–1O and Supplemental Figure 2B). Therefore, inner ovary walls of 11-DPA capsules were collected for protoplast isolation (Figure 1P–1Q). Samples with approximately 20 000 protoplasts were prepared and immediately mixed with 10x Genomics single-cell reaction reagents and cell barcodes. Processed samples were then used for library construction and sequencing on the 10x Genomics scRNA-seq platform (Figure 1R).

scRNA-seq and cell-type cluster identification

Transcriptome data were obtained from 16 000 valid single cells using the 10x Genomics scRNA-seq platform (Supplemental Figure 3). To ensure the quality of the single-cell data, only cells with gene counts between 300 and 6000 were retained (Supplemental Figure 4A), and cells with more than 20 000 unique molecular identifiers (UMIs) were removed (Supplemental Figure 4B). Finally, 15 567 high-quality cells were retained, and 43 450 genes were identified, with an average of 3167 UMIs and 1896 genes per cell (Supplemental Table 1). The 15 567 single cells were classified into 10 clusters by unsupervised clustering analysis, and the data were visualized

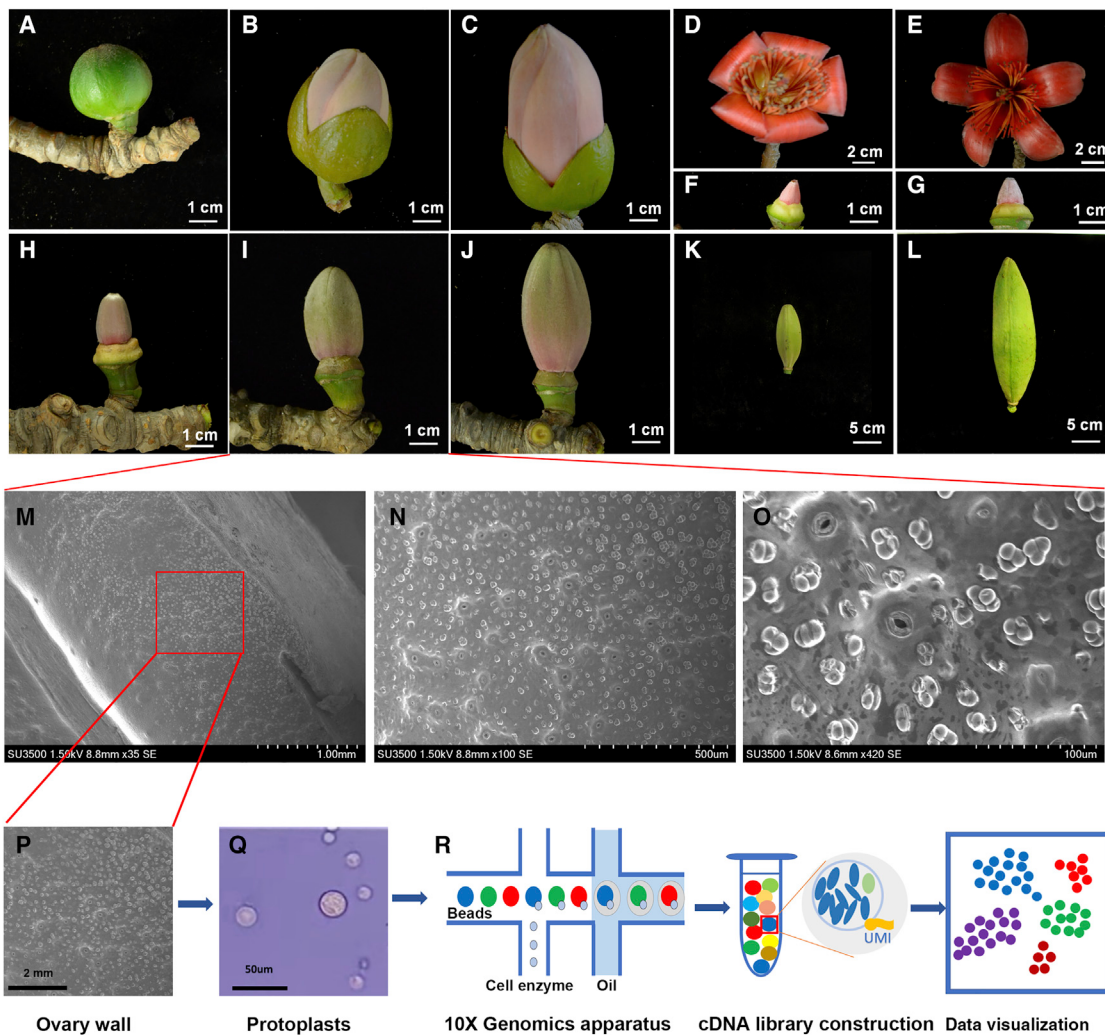


Figure 1. Identification and application of scRNA-seq in fibre initiation of *B. ceiba*.

(A–L) The development of the flower and capsule in *B. ceiba*: (A–E) development processes of flowers at –10, –3, –1, 0, and 3 days post anthesis (DPA); (F–L) development processes of capsules at 8, 11, 14, 16 and 30 DPA.

(M–O) Scanning electron microscopy (SEM) of the 11 DPA *B. ceiba* inner wall. Scale bars: 1 mm in (M); 500 μ m in (N); 100 μ m in (O).

by Uniform Manifold Approximation and Projection (UMAP) (Figure 2A). The number of cells varied among clusters, from cluster 0 with 6958 cells (45.49%) to cluster 9 with 37 cells (0.24%) (Figure 2B).

We sought to identify two specific cell types associated with *B. ceiba* fiber initiation: initiated fiber cells and inner ovary wall epidermal cells. Marker genes specifically expressed in initiated fiber cells of cotton were used to identify the initiated fiber cell cluster in *B. ceiba*; these included *MYBMIXTA-Like 4* (*MML4*) (Tian et al., 2020), *MYB25* (Machado et al., 2009), *HD-ZIP homeobox 3* (*HOX3*) (Shan et al., 2014), *DEL65* (Shangguan et al., 2016), *HD1* (Walford et al., 2012), and *PDF1* (Deng et al., 2012). The homologous *B. ceiba* genes were specifically expressed in cluster 6 (Figure 2C). Likewise, marker genes involved in differentiation of stomatal guard cells and inhibition of fiber initiation, such as *CPC* (Liu et al., 2015), *HIC* (Gray et al., 2000), *MYB61* (Liang et al., 2005), *FLP* (Lai et al., 2005),

and *CUT1* (Millar et al., 1999), were found in cluster 3 (Figure 2C and Supplemental Table 2). RNA *in situ* hybridization with four representative genes (*HD1*, *TUA9*, *CPC*, and *CUT1*) from cell clusters 3 and 6 provided additional support for the annotation of these clusters as epidermal and fiber cells (Figure 2D). Thus, cells from cluster 6 were initiated fiber cells, and cells from cluster 3 were epidermal cells of the inner ovary wall.

Identification of marker genes involved in *B. ceiba* fiber initiation

To identify the specific marker genes involved in *B. ceiba* fiber initiation, 347 specifically expressed genes (SEGs) were identified in fiber initiation cell cluster 6 (FICC6) (Supplemental Table 3). The expression levels of the top 54 most highly expressed genes are depicted as a heatmap (Figure 3A); these genes were specifically expressed in FICC6. Six highly expressed

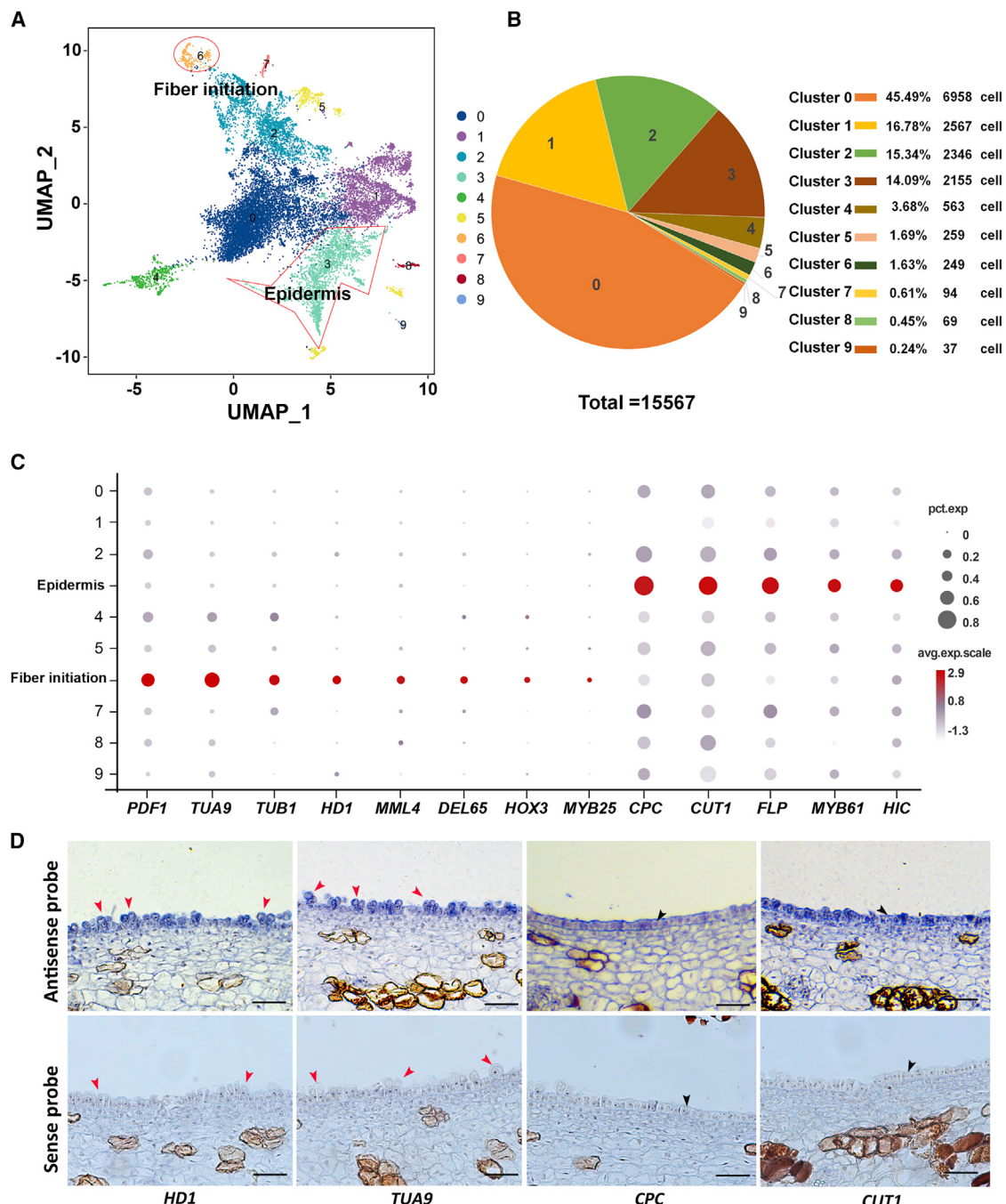


Figure 2. Identification and application of scRNA-seq in fibre initiation of *B. ceiba*.

(A) Uniform manifold approximation and projection (UMAP) visualization of 10 cell clusters. Individual cells are represented by dots; n = 15567; cell clusters are coloured differently.

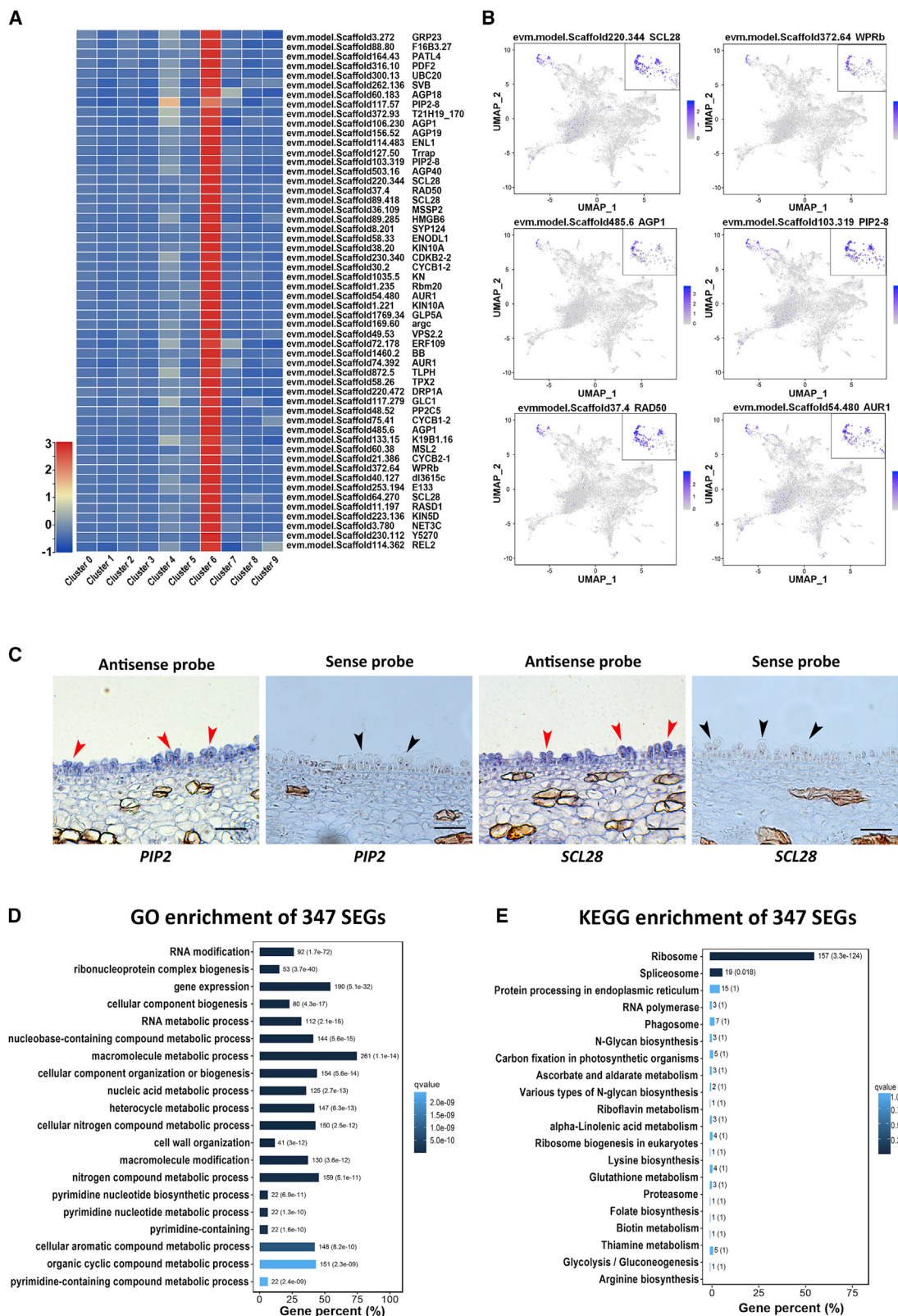
(B) Number and percentage of cells in each cluster.

(C) Expression patterns of cluster-specific marker genes. The size of the circle represents the percentage of cells with expression (pct.exp.), and the colour represents the average expression after scaling (avg.exp.scale).

(D) RNA *in situ* hybridization of HD1, TUA9, CPC and CUT1 in 11 DPA capsules with the sense probe as a negative control. Red arrows indicate fibre cells, and black arrows indicate non-fibre epidermic cell. Scale bar, 50 µm.

representative genes from FICC6 (*SCL28*, *WPRB*, *AGP1*, *PIP2-8*, *RAD50*, and *AUR1*) are displayed in UMAP map clusters (Figure 3B). We found that these genes were most highly expressed and concentrated in FICC6. RNA *in situ* hybridization with *PIP2* and *SCL28* confirmed their gene expression patterns

in FICC6 (Figure 3C). Gene ontology (GO) and Kyoto Encyclopedia of Genes and Genomes (KEGG) analyses suggested that the 347 SEGs from FICC6 were enriched mainly in RNA modification, ribonucleoprotein complex biogenesis, and the ribosome pathway (Figure 3D and 3E).

**Figure 3. Identification of a new marker gene for fibre initiation clusters in *B. ceiba*.**

(A) Heatmap showing the top specifically expressed genes (SEGs) with the highest expression levels (log₂fold change) in the fibre initiation cluster.

(B) Expression patterns of six new marker genes on the UMAP map.

(legend continued on next page)

Differentiation trajectory of initiated fiber cells from the epidermis

The ability of scRNA-seq to capture cells in different developmental states makes it possible to study successive differentiation trajectories during tissue or cell development. To further explore the developmental processes of initiated fiber cells, pseudotime trajectory analysis was performed using cell clusters 3 (inner wall epidermis) and 6 (initiated fiber cells) in **Figure 2A**. For fibers that developed from the epidermis, the epidermal cell cluster was considered the origin of the developmental trajectory, and the bifurcation point marked cells with changes in differentiation state (**Figure 4A**). The pseudotime trajectory showed that cells eventually differentiated into two cell types: differentiated epidermal cells (branch 1) and initiated fiber cells (branch 2) (**Figure 4A** and **4B** and [Supplemental Figure 5](#)). To further classify the cell types of branches 1 and 2, expression levels of the epidermal marker gene *HIC* and the fiber initiation marker gene *PDF1* are shown in the branches. *HIC* was found at the end of branch 1 (**Figure 4C**) and is mainly involved in differentiation of mature stomatal guard cells, whereas *PDF1* was mainly found at the end of branch 2 (**Figure 4D**) and is related to fiber initiation. Expression patterns of six more genes from branches 1 and 2 further supported the cell-type classifications of these branches ([Supplemental Figure 6](#)). Cells from epidermal and initiated fibers were continuously distributed along branch 2 (**Figure 4B**), demonstrating that pseudotime analysis essentially revealed the development of fiber initiation. The top 10 SEGs involved in cell differentiation from epidermal cells to other tissues or fiber cells are shown in **Figure 4E**. These genes may play a role in the differentiation of stomata and fiber initiation cells from the inner epidermis of the ovary.

The expression levels of all SEGs of inner wall epidermal cells (branch 1) and fiber initiation cells (branch 2) are shown in a heatmap (**Figure 4F**), and the SEGs were classified into five modules (M1–5) according to their expression profiles ([Supplemental Table 4](#)). Genes from M1 and M2 were extremely highly expressed in cells from the ends of branches 1 and 2 (**Figure 4E**), suggesting that these genes functioned in the processes of stomatal cell differentiation and fiber initiation, respectively. Genes from M4 were highly expressed in cells of the prebranch, indicating that they may help to maintain the undifferentiated state of primitive epidermal cells or to prepare for the differentiation stage. Genes from M3 and M5 were more highly expressed in cells of the transition state, implying that they probably functioned in the differentiation of fiber cells or stomatal cells. GO analysis of genes from M1–5 showed that genes in M2 were mainly enriched in structural molecule activity and ribosome-related processes (**Figure 4F**) and possibly functioned in differentiated fiber cell growth. On the other hand, genes from M1 and M5 were enriched in phenylpropanoid metabolic processes and ubiquitin-like protein ligase binding processes, respectively, and genes from M3 and M4 were mainly involved in response to stimuli (**Figure 4F**). GO analysis thus showed that genes from different modules were enriched in

specific biological processes, implying that strict temporal and spatial regulation of gene expression determines the direction of epidermal cell differentiation in *B. ceiba*.

Fiber initiation is controlled by many TFs. To identify TFs that potentially regulate fiber initiation in *B. ceiba*, we identified those that were specifically expressed in the inner wall epidermal cell cluster and the initiated fiber cell cluster. In total, 528 TFs were identified, and members of the MYB (43 genes) and bHLH families (54 genes) were the most highly specifically expressed TFs in the initiated fiber cell cluster ([Supplemental Figure 7](#) and [Supplemental Table 5](#)). All identified TFs were used to construct a regulatory network showing their relationships (**Figure 4G**). Within this network were some important TFs reported to participate in fiber initiation, such as *HD1* (Walford et al., 2012), *BZR1* (Zhou et al., 2015), *MYB2* (Wang et al., 2004), *TRY* (Liu et al., 2015), and *HOX1* (Huang et al., 2021) (**Figure 4G**). Several TFs strongly related to cell division were also found, such as *WOX3* (Shimizu et al., 2009), *DOF3.4* (Skirycz et al., 2008), *SCL28* (Goldy et al., 2021), and *MYB88* (Yang et al., 2014) (**Figure 4G**), as were fiber development- or elongation-related TFs such as *SLR1* (Ueguchi-Tanaka et al., 2008), *MYB106* (Jakoby et al., 2008), *ETC1* (Kirik et al., 2004), *PDF2* (Qin et al., 2022), and *GEBPL* (Shaikhali et al., 2015) (**Figure 4G**). Specifically expressed TFs in the fiber initiation cluster were then subjected to GO and KEGG enrichment analysis. The cell cycle process was the most enriched GO biological process ([Supplemental Figure 8A](#)), and enrichment of the ribosome, spliceosome, and starch and sucrose metabolism pathways was revealed by KEGG pathway analysis ([Supplemental Figure 8B](#)).

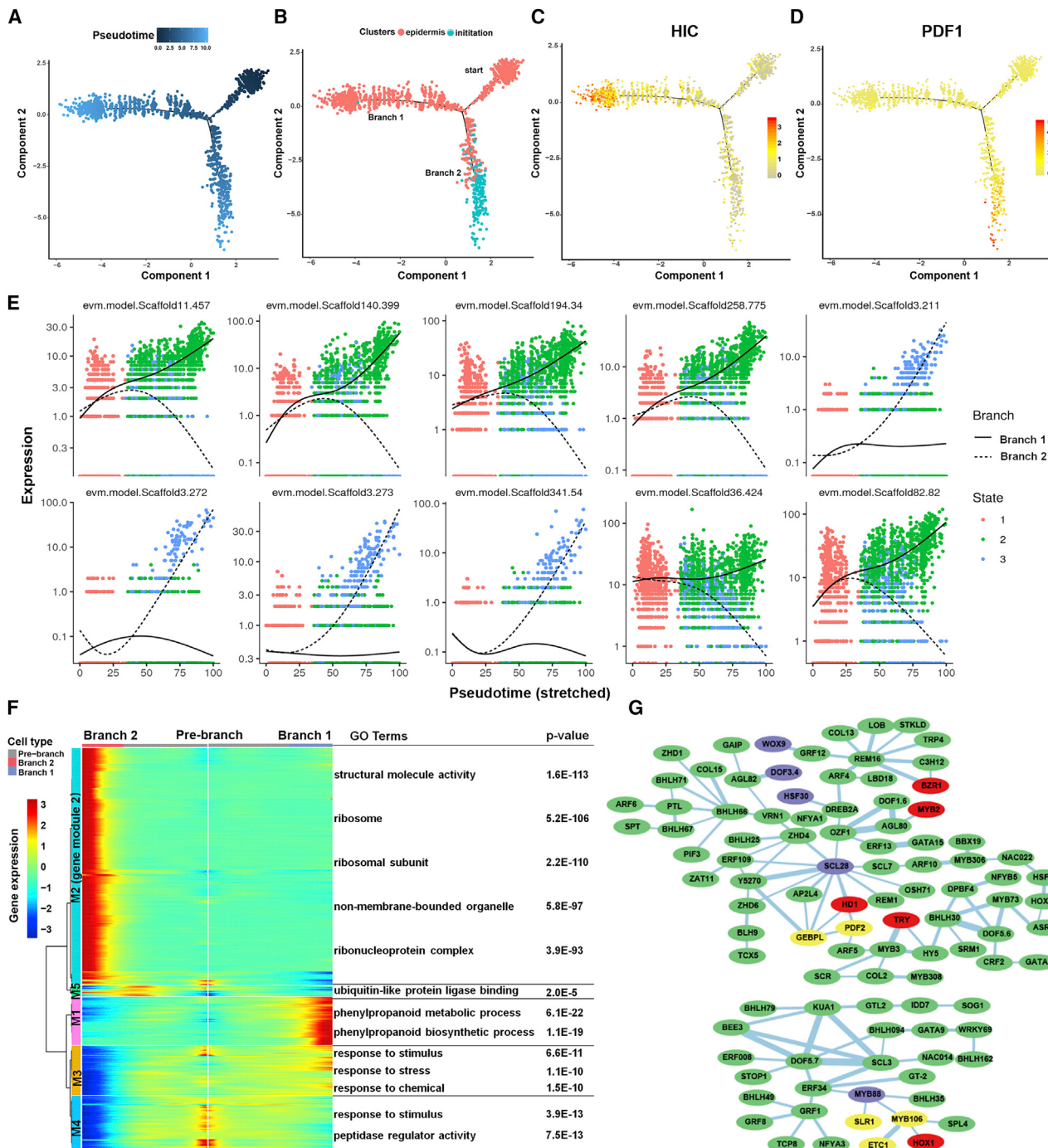
Similarities and differences in fiber initiation between cotton and *B. ceiba*

Cotton fibers originate from the outer epidermal cells of the ovule, whereas *B. ceiba* fibers differentiate from the epidermis of the inner ovary wall. To explore the evolutionary conservation and differences in fiber cell initiation between cotton and *B. ceiba*, we performed an integrated analysis with single-cell datasets of initiated fiber cells from *G. hirsutum* (TM-1) (Qin et al., 2022) and *B. ceiba*. A total of 518 SEGs related to cotton fiber initiation were identified in the single-cell dataset from epidermal cells of cotton ovules ([Supplemental Table 7](#)). These 518 SEGs were aligned to the *B. ceiba* genome, revealing 277 orthologous genes ([Supplemental Table 8](#)). Of the 347 SEGs identified in FICC6 of *B. ceiba*, only 74 were shared with cotton (**Figure 5A**). By contrast, 203 and 273 SEGs were specifically expressed in cotton and *B. ceiba* FICC6, respectively ([Supplemental Tables 8](#) and [9](#)), and were then used for GO enrichment analysis. Most SEGs from cotton and *B. ceiba* were enriched in the same biological processes, but only SEGs from *B. ceiba* were enriched in mitotic cytokinesis and cell division (**Figure 5B** and **5C**). In contrast to cotton fibers, initiated fiber cells of *B. ceiba* undergo continuous mitosis, producing many initiated cell clusters on the epidermis of the inner ovary wall,

(C) RNA *in situ* hybridization of *PIP2* and *SCL28* in 11 DPA capsules with the anti-sense probes, and sense probes were used as negative controls. Red arrows indicate staining fibre cells, and black arrows indicate unstaining fibre cells from negative controls. Scale bar, 50 µm.

(D) GO enrichment analysis of all SEGs in the fibre initiation cluster.

(E) KEGG enrichment analysis of all SEGs in the fibre initiation cluster.

**Figure 4. Differentiation trajectory of epidermis and fibre initiation.**

(A) Pseudotime trajectory of fibre initiation and epidermal cell development. Each dot indicates a single cell.

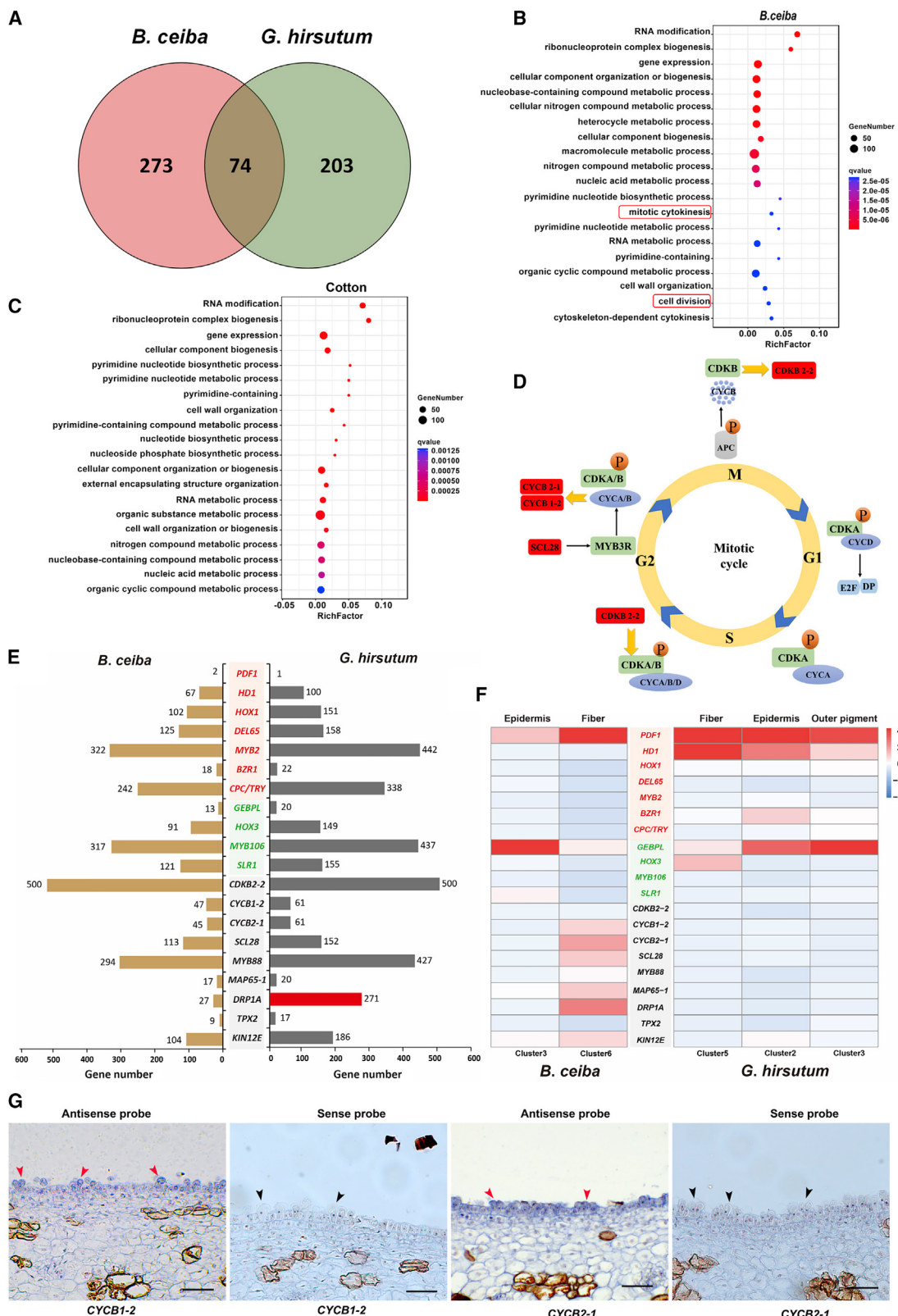
(B) Pseudotime trajectory of single-cell transcriptomics data coloured according to cluster. Each dot indicates a single cell.

(C-D) Expression of marker genes by cell type on a pseudotemporal trajectory. Colours indicate gene expression level in individual cells.

(E) Pseudotime expression trajectories of branch-dependent top 10 SEGs. Branch 1 indicates the differentiation directions to epidermic cell, and initiated fibre cell of Branch 2. State 1-3 represent three differentiated situations of single cells.

(F) Trends in gene expression with branching in cells based on different differentiation fates. The GO term enriched significantly in each cluster is shown on the right.

(G) A transcription factor (TF) regulatory network constructed by all identified TFs from initiated fibre cell clusters and epidemic cell clusters. Red blocks represent TFs reported associate to fibre initiation; yellow blocks show TFs related to fibre development or elongation; purple blocks mean TFs related to cell division. Line thickness indicates the strength of association between TFs.

**Figure 5. Evolutionary conservation and divergence of fibre initiation cell types in cotton and *B. ceiba*.**(A) Venn diagram showing the number of homologous and SEGs in *B. ceiba* and cotton fibre initiation cell types.(B-C) GO analysis of genes specifically expressed in *B. ceiba* and cotton.

(legend continued on next page)

which then elongate into mature fibers (Supplemental Figure 2B). SEGs related to cell division in *B. ceiba* included CYCB2-1 (Lee et al., 2003), CYCB1-2 (Romeiro Motta et al., 2022), CDKB 2-2 (Andersen et al., 2008), MYB88 (Yang et al., 2014), and SCL28 (Goldy et al., 2021), all of which participate in the mitotic cycle of plant cells (Figure 5D). SCL28 was located in the center of the TF network and is related to the known important regulator HD1 (Figure 4G). Thus, we speculate that SCL28 may have an important role in cell cluster formation during fiber initiation in *B. ceiba*.

To further analyze differences in fiber initiation between *B. ceiba* and cotton at the genome level, we identified gene family expansions and contractions of key fiber initiation regulators in *B. ceiba* and *G. hirsutum* and analyzed their expression differences at the single-cell level (Figure 5E and 5F). Most of these gene families were expanded in *G. hirsutum* compared with *B. ceiba*, especially DRP1A (red bar), which has 271 members in *G. hirsutum*, 10 times more than in *B. ceiba* (Figure 5E). Heatmap analysis showed that cell division-related genes (black font) were highly expressed in the *B. ceiba* fiber cell cluster compared with cotton, which is consistent with differences in fiber initiation between the two species; i.e., initiated fiber cells of *B. ceiba* undergo additional cell divisions that do not occur in cotton (Figure 5F). Some genes with previously reported functions in fiber initiation (red font) were highly expressed in the fiber cell cluster (Supplemental Table 10). We performed RNA *in situ* hybridization with CYCB1-2 (Romeiro Motta et al., 2022) and CYCB2-1 (Lee et al., 2003) to validate the expression patterns of cell division-related genes in the *B. ceiba* ovary and found that these genes were highly expressed in initiated fiber cells (Figure 5G).

Initiation process of fiber cells in *B. ceiba*

A summary of the regulatory factors associated with fiber initiation in *B. ceiba* is shown in Figure 6. Like cotton fiber development, *B. ceiba* fiber development comprises three stages: fiber initiation, elongation, and maturation. In cotton, fiber cells initiate from seed epidermal cells and enter the elongation stage directly. By contrast, *B. ceiba* fiber cells undergo an extra cell division process after differentiation from the epidermal cells of the inner ovary wall, resulting in a series of fiber cell clusters (Figure 1O and Supplemental Figure 2B) that subsequently elongate into long fiber cells. SEGs from *B. ceiba*, including PDF1 (Deng et al., 2012), HD1 (Walford et al., 2012), HOX1 (Huang et al., 2021), DEL65 (Shangguan et al., 2016), MYB2 (Wang et al., 2004), BZR1 (Zhou et al., 2015), and CPC/TRY (Liu et al., 2015), are known to function in fiber initiation in cotton. In this study, we suspected that GEBPL (Shaikhali et al., 2015), HOX3 (Shan et al., 2014), MYB106 (Jakoby et al., 2008), and SLR1 (Ueguchi-Tanaka et al.,

2008) might be involved in fiber initiation in *B. ceiba*. The primary initiated fiber cells of *B. ceiba* continue to divide into multicellular groups, and cell cycle regulators such as CDKB2-2 (Andersen et al., 2008), CYCB1-2 (Romeiro Motta et al., 2022), CYCB2-1 (Lee et al., 2003), SCL28 (Goldy et al., 2021), and MYB88 are considered to function in fiber initiation of *B. ceiba*. Enriched microtubule-associated proteins such as MAP65-1 (Smertenko et al., 2006), DRP1A (Mravec et al., 2011), TPX2 (Bird and Hyman, 2008), and KIN12E (Herrmann et al., 2021) may also participate in fiber cell mitosis during this process. Once fiber initiation is complete, fiber cells transition to the elongation stage.

DISCUSSION

Traditional transcriptome sequencing techniques measure the average expression levels of genes in a population of cells, precluding accurate assessment of gene expression in individual cells or cell types and thus obscuring the heterogeneity of expression among different cells (Tang et al., 2011). Single-celled natural fibers, including those of cotton and cottonwood, are the best material for studying single-cell differentiation and development. scRNA-seq is an excellent method for investigating the molecular mechanisms that underlie fiber cell initiation and development at the single-cell level. The natural fibers of *B. ceiba* have unique properties and specific developmental processes not found in cotton fibers, indicating the presence of a species-specific regulatory network and offering potential genetic resources for research on fiber development. Using scRNA-seq to study the initiation of cotton fiber cells can provide important reference data and new genetic resources for fiber initiation in cotton.

Characteristics of natural fiber differentiation

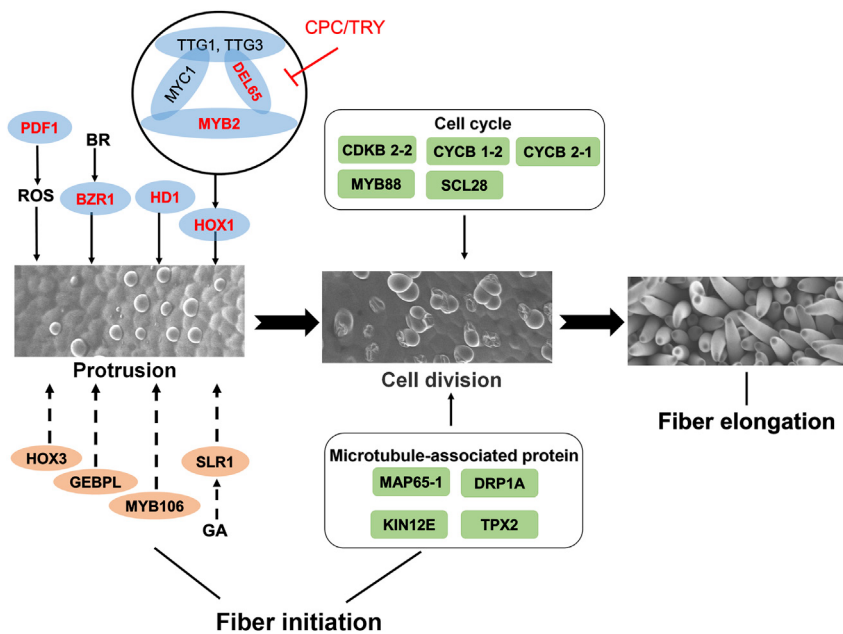
Based on scRNA-seq combined with GO and KEGG enrichment analyses, 347 SEGs were identified in *B. ceiba* FICC6 and found to be strongly enriched in ribosome-related pathways (Figure 3D and 3E). Previous studies have shown that the nucleus is significantly enlarged in epidermal cells that differentiate into fiber-initiating cells (de Moura et al., 2020), indicating that ribosomal RNA (rRNA) biosynthesis is necessary for fiber cell differentiation (Bahadori, 2019). In a recent cotton scRNA-seq study (Qin et al., 2022), the GO terms “regulation of ethylene-activated signalling pathway,” “sucrose alpha-glucosidase activity,” and “cuticle hydrocarbon biosynthetic process” were enriched in a gene module analysis of cotton fiber initiation, and these terms were previously reported to be enriched during cotton fiber elongation (Shi et al., 2006). Our pseudotime analysis showed that the epidermis differentiated into two main cell types: initiated fiber cells and differentiated epidermal cells (Figure 4A and 4B). A large number of guard cells are distributed on the epidermis of the inner ovary wall

(D) Specific expression of *B. ceiba* genes in cell cycle regulation. Four stages of cell mitotic cycle are Gap1 (G1), Synthesis (S), Gap2 (G2) and Mitotic (M). The complexes surround mitotic cycle are regulators for each stage. The specific genes found in *B. ceiba* initiated fibre cell clusters are marked in red.

(E) Gene family expansion and contraction in *B. ceiba* and *G. hirsutum*. Red blocks showed extremely more members found in *G. hirsutum* of DRP1A gene family. Gray and brown blocks represent gene numbers of gene family. Red, green and black font gene names represent genes reported function in fibre initiation, speculative function in fibre initiation and related to cell division process, respectively.

(F) Heatmap showing the expression level of representative genes at single-cell level in fibre and epidermic cell clusters in *B. ceiba* and *G. hirsutum*. Meaning of red, green and black font gene names were the same as above description.

(G) RNA *in situ* hybridization of two cell division related genes, CYCB1-2 and CYCB2- 1 in 11 DPA capsules with the sense (negative control) and antisense probes. Red arrows indicate staining fibre cells, and black arrows indicate unstaining fibre cells from negative controls. Scale bar, 50 μ m.



surface of *B. ceiba* (Supplemental Figure 2B). In cotton, ovule epidermal cells can also develop into fibers and stomata (James Mc, 1975). Here, the marker gene *HIC* (Gray et al., 2000), which has been reported to function in stomatal development, was highly expressed in differentiated epidermal cell clusters (Figure 4C, Branch 1). Thus, natural fiber initiation involves at least two developmental trajectories: initiated fiber cells and stomatal cells.

Genes associated with the differentiation of *B. ceiba* fiber cells

The initiation of fiber development is a complex process whose molecular regulatory mechanisms remain to be fully clarified. Some important genes such as *HD1* and *MYB25* have been shown to play essential roles in cotton fiber initiation, but very little is known about the analogous process in *B. ceiba*. In cotton, fiber initiation is regulated by many TFs such as R2R3-MYB (*GhMML4* and *GhMYB25*) (Machado et al., 2009; Tian et al., 2020), bHLH (*GhDEL65*) (Shangguan et al., 2016), and HD-ZIP IV (*GpPDF1* and *GhHD1*) (Deng et al., 2012; Chen et al., 2017). Here, their orthologs were specifically expressed in FICC6 of *B. ceiba* (Figure 2C), indicating that the fiber initiation mechanisms of cotton and *B. ceiba* share some similarities. Orthologs of other cotton TFs such as TRY (Ishida et al., 2008), BZR1 (Zhou et al., 2015), MYB2 (Wang et al., 2004), and HOX1 (Huang et al., 2021), which are involved in regulating cotton fiber initiation, were also specifically expressed in FICC6 of *B. ceiba* (Figure 4G). In *Arabidopsis*, the TRY protein has been shown to move to neighboring cells and compete with GL1 for GL3/EGL3 binding, resulting in inhibition of trichome development (Ishida et al., 2008). In this study, TRY was expressed in FICC6 of *B. ceiba* (Figure 4G), indicating that it also functions in *B. ceiba*'s fiber initiation process. Some other TFs whose genes were specifically expressed in *B. ceiba*, such as SLR1 (Ueguchi-Tanaka et al., 2008), MYB106 (Jakoby et al., 2008), HOX3 (Shan et al., 2014), and GEBPL (Shaikhali et al., 2015), were found to interact with these reported genes in the

Special fiber initiation process in *B. ceiba*

Figure 6. Schematic diagram of gene regulation related to cell differentiation and development in *B. ceiba*-initiating fibres.

Early developmental process of *B. ceiba* are divided into three stages including protrusion, cell division and elongation; protrusion and cell division stages are together composed the fibre initiation process. Regulators and network upon 'Protrusion' block are reported proteins involved in fibre initiation process, proteins with red markers were proteins found in *B. ceiba*. Regulators under 'Protrusion' block are suspected proteins that potential related to the fibre initiation of *B. ceiba* according to the network analysis in Figure 4G that strong connected with the reported regulators. Reported regulators related to 'Cell division' were divided into cell cycle and microtubule-associated types and marked with green blocks.

regulatory network (Figure 4G). In cotton, GhSLR1 is a blocker of the phytohormone gibberellic acid; it interferes with stabilization of the GhHOX3-GhHD1 complex, inhibits transcription of downstream target genes, and ultimately suppresses fiber elongation (Shan et al., 2014). GEBPL encodes a GLABROUS1 enhancer-binding protein that promotes trichome generation (Curaba et al., 2003). GL1 is an important regulator of the MYB-bHLH-WD40 (MBW) ternary complex in *Arabidopsis*, controlling the production of trichomes (Larkin et al., 1994). Thus, we suspect that *GEBPL*, *MYB106*, *HOX3*, and *SLR1* play important roles in fiber initiation of *B. ceiba*.

Similarities and differences in fiber initiation of cotton and *B. ceiba*

There are two major similarities between *B. ceiba* fibers and cotton fibers: both are single cells generated from epidermal cells, and both undergo a similar developmental process that includes initiation, elongation, and dehydration. Many key regulators of cotton fiber initiation were also expressed during fiber initiation in *B. ceiba*, including *PDF1*, *TRY*, *BZR1*, *HD1*, *HOX1*, and *HOX3*, indicating that fiber initiation in the two species involves similar regulatory mechanisms. However, there are also two main differences in fiber initiation between cotton and *B. ceiba*. First, fibers of *B. ceiba* originate from epidermal cells of the inner ovary wall (Figure 1M-1O and Supplemental Figure 2B), and second, the initiated fiber cells of *B. ceiba* undergo cell division and form clusters of single fiber cells that eventually develop into mature fibers (Figure 1M-1O and Supplemental Figure 2B). Cotton fibers are individual cells initiated from outer epidermal cells of the ovule that elongate and dehydrate to become mature fibers (Stewart, 1975). Here, gene expression profiling revealed that SEGs in FICC6 from *B. ceiba* were enriched in GO terms related to mitosis and cell division (Figure 5B), and TF network analysis indicated that the cell cycle TF *SCL28* might be an important regulator of cell cluster generation (Figure 4G). *SCL28* belongs to the GRAS family (Goldy et al., 2021); it accumulates during the G2/M phase of the cell cycle, facilitates the progression of cell division through G2/M, and regulates the selection of cytokinesis planes (Goldy et al., 2021). Other SEGs related to the cell cycle or mitotic cytokinesis, such as

CYCB2-1, *CYCB1-2*, *CDKB2-2*, and *MAP65-1*, were uniquely expressed in *B. ceiba* FICC6 (Figure 6). CYCBs have been reported to regulate the G2/M transition and induce mitotic cycles in endoreduplicating *Arabidopsis* cells (Schnittger et al., 2002), and the cyclin-dependent kinase *CDKB2-2* is essential for normal cell cycle progression and meristem integrity (Andersen et al., 2008). Cell division depends on the control of microtubule dynamics and organization (Banerjee et al., 2020). *MAP65-1* has been shown to have a cell cycle-dependent microtubule binding pattern (Smertenko et al., 2006), and it was specifically expressed in FICC6 of *B. ceiba*. In conclusion, fiber initiation in cotton and *B. ceiba* involves similar regulatory mechanisms, but *B. ceiba* fiber initiation also involves cell division and corresponding regulators, which may be applicable for improvement of fiber yield in cotton.

METHODS

Observation of *B. ceiba* fiber initiation

Plant materials were collected from *B. ceiba* trees (>10 years of age) planted on the campus of Hainan University in Haikou, China (20°3'23.07"N, 110°19'29.388"E). To confirm the timing of fiber initiation in *B. ceiba*, capsules were photographed from 0 DPA to 11 DPA using an SU3500 scanning electron microscope (Hitachi, Japan) in order to observe the numbers of initial cells on the inner ovary walls. Mature fibers of *B. ceiba* form fiber agglomerates that facilitate seed dispersal by the wind. Mature capsules of *B. ceiba* were collected from five different plants, and more than 200 fiber agglomerates were randomly selected from each plant for fiber length measurements.

Protoplast isolation from the inner ovary wall of *B. ceiba*

All 11-DPA capsules of *B. ceiba* were observed by scanning electron microscopy to ensure that fiber cells had been initiated. Selected capsules were dissected, ovules were removed, and the innermost ovary wall layers were obtained and cut into 1- to 2-mm strips. Samples were then placed in a tube containing 20 ml of enzyme solution (2% [w/v] Cellulase R10; 1% [w/v] Macerozyme R10; 1% hemicellulase; 20 mM MES, pH 5.7; 0.5 M mannitol; 20 mM KCl; 10 mM CaCl₂; 0.1% BSA [w/v]). After digestion at 26°C with shaking at 25 rpm for 4 h, an equal volume of PBS solution (without calcium and magnesium) was added to the tube, and the tube was gently shaken to release the protoplasts. Protoplasts were then filtered through a 40-μm nylon mesh, centrifuged at 300 g for 5 min at 4°C, and washed three to four times with PBS solution. A small amount of single-cell suspension was taken, and an equal volume of 4% Trypan blue was added for viability determination. Samples were considered acceptable if the percentage of viable cells was greater than 85% of the total cell number. The cells were counted with a Countess II Automated Cell Counter, and the live cell concentrations were adjusted to 1500 to 2000 cells/μl.

scRNA-seq library construction

scRNA-seq libraries were sequenced on the Illumina sequencing platform by Gene Denovo Biotechnology (Guangzhou, China). Protoplasts were loaded onto a 10x Genomics Chromium Controller to generate single-cell gel beads in emulsion (GEMs) in which lysis and barcoded reverse transcription of mRNA were performed. The products of all GEMs were mixed, and a standard sequencing library was constructed. The cDNA was amplified by PCR using the sequencing primers R1 and R2 and ligated to Illumina sequencing adapters for the P5 and P7 flow-cell binding sites. High-throughput sequencing of the constructed libraries was performed on the Illumina sequencing platform to generate 150-bp paired-end reads.

scRNA-seq data processing and analysis

The scRNA-seq data were aligned to the *B. ceiba* reference genome (Sequence Read Archive PRJNA429932) (Gao et al., 2018). Raw

scRNA-seq data were aligned, filtered, and normalized using Cell Ranger 3.1.0 software (10x Genomics), resulting in a gene expression matrix for each cell. The Seurat (v3.1.0) R toolkit was used to explore QC indicators, filter cells, visualize gene and molecular counts, plot their relationships, and exclude cells with clearly abnormal numbers of gene tests as potential multiples (Butler et al., 2018). Data normalization was performed using the global-scaling normalization method "LogNormalize" (Risso et al., 2014). To overcome the extensive technical noise for any single gene in scRNA-seq data, we used the UMAP method to place cells with similar neighborhoods in high-dimensional space into lower dimensional space for data visualization (Becht et al., 2018).

Analysis of SEGs

To analyze patterns of transcriptional regulation in individual cell subsets, likelihood-ratio tests were performed to identify SEGs in individual cells and compare them with all other cells. SEGs were identified using the following parameters: *p* value ≤ 0.01, log₂FC ≥ 0.36, and percentage of cells in which the gene was detected in a specific cluster >25%. GO enrichment analyses were performed based on gene expression levels to identify the main functions of the clusters. To analyze marker genes of the initiation cluster, we selected the top genes according to the results of the SEG analysis and used TBtools to draw a gene expression heatmap (Chen et al., 2020).

Pseudotime trajectory analysis

The Monocle package (version 3.0) was used to construct cell differentiation trajectories for selected clusters (Trapnell et al., 2014). The trajectory was visualized as a tree-like structure with tips and branches. Gene expression profiles in Monocle were used to identify genes that were specifically expressed between groups of cells and to assess the statistical significance of those findings (Qiu et al., 2017). Pseudotime analysis of fiber development was performed, and genes with similar expression trends were grouped. The branch point was selected to identify genes that contributed to branching of the developmental trajectory. The differential gene test function was used to identify pseudotime-dependent and branch-dependent genes. Genes that were significantly branch dependent were visualized using the plot-genes-branched-heatmap function.

RNA *in situ* hybridization

RNA *in situ* hybridization experiments were carried out as described previously (Zhang et al., 2017). In brief, gene-specific probes were prepared as described in the manual of the DIG Northern Starter Kit (Roche); primers used in this study are listed in Supplemental Table 11. Samples were prepared from 11-DPA capsules of *B. ceiba* and embedded in paraffin for later use; 10-μm paraffin sections were obtained, deparaffinized, rehydrated, and incubated overnight with the RNA probe in darkness. After a series of washes with SSC (saline–sodium citrate) and NTE (0.5 M NaCl, 10 mM Tris [pH 8.0], 1 mM EDTA) buffers, the non-specifically bound probe was removed. Alkaline phosphatase-conjugated anti-digoxigenin (anti-Dig-AP, Roche) and nitro-blue tetrazolium/5-bromo-4-chloro-3-indol-phosphate (NBT/BCIP) color substrate solution (Roche) were used for color development. Ovary sections of *B. ceiba* were photographed using a CX33 microscope (Olympus, Tokyo, Japan) in bright-field mode.

Comparative analysis of fiber initiation-related gene clusters generated by scRNA-seq in *G. hirsutum* and *B. ceiba*

scRNA-seq data from the outermost layer of cotton ovules were recently published by the Group of Cotton Genetic Improvement, National Key Laboratory of Crop Genetic Improvement, Huazhong Agricultural University, Wuhan, Hubei, China2 (Qin et al., 2022). To investigate the similarities and differences in fiber development between *B. ceiba* and cotton, orthologous genes were first identified by blasting the 518 SEGs in the cotton FICC against *B. ceiba* protein sequences with an *e*-value threshold of 1e⁻⁵. To analyze gene family expansion and contraction,

protein sequences were obtained from the *G. hirsutum* TM-1 genome (Wang et al., 2019) and the *B. ceiba* genome (Gao et al., 2018); gene family members were identified using blast tools under the screening condition of *p* value <10⁻⁵.

DATA AVAILABILITY

The raw sequencing data are available at the National Center for Biotechnology Information Sequence Read Archive under BioProject accession number PRJNA850395 and the China National Genomics Data Center (<https://ngdc.cncb.ac.cn>) under BioProject accession number PRJCA014500.

SUPPLEMENTAL INFORMATION

Supplemental information is available at *Plant Communications Online*.

FUNDING

This work was supported by the National Natural Science Foundation of China (31960437).

AUTHOR CONTRIBUTIONS

H.Y.H. and Y.H.D. conceptualized and designed the experiments. X.P.L. performed most of the experiments under the supervision of H.Y.H. and guidance of Y.H.D. W.G., Y.Q., and Z.N.Z. completed the RNA *in situ* hybridization experiments, and Y.H.D. captured the figures. W.J.L., K.G., and S.H.Z. helped to collect the samples. Y.Y. and P.L. provided help with bioinformatics analysis. Y.H.D. and X.P.L. wrote the manuscript with the support of all other authors. K.G., Y.Y., and H.Y.H. critically revised the manuscript. W.G. and Y.Q. added the RNA *in situ* hybridization experiment.

ACKNOWLEDGMENTS

The support for Kai Guo and Yong Yang in writing the manuscript is greatly appreciated. We thank Wenjie Lai and Sihan Zhou for support with sample collection and protoplast isolation. Thanks to Kai Guo for help with sample observation by scanning electron microscopy and Yong Yang and Ping Li for support with bioinformatics analysis. We also thank Wei Gao, Yuan Qin, and Zhennan Zhang for help with the RNA *in situ* hybridization experiments. We show our appreciation to Guangzhou Gene Denovo Biotechnology Co., Ltd. for support with single-cell sequencing. No conflict of interest is declared.

Received: August 7, 2022

Revised: December 19, 2022

Accepted: January 20, 2023

Published: February 10, 2023

REFERENCES

- Andersen, S.U., Buechel, S., Zhao, Z., Ljung, K., Novák, O., Busch, W., Schuster, C., and Lohmann, J.U. (2008). Requirement of B2-type cyclin-dependent kinases for meristem integrity in *Arabidopsis thaliana*. *Plant Cell* **20**:88–100. <https://doi.org/10.1105/tpc.107.054676>.
- Bahadori, M. (2019). New insights into connection of nucleolar functions and cancer. *Tanaffos* **18**:173–179.
- Banerjee, G., Singh, D., and Sinha, A.K. (2020). Plant cell cycle regulators: mitogen-activated protein kinase, a new regulating switch? *Plant Sci.* **301**:110660. <https://doi.org/10.1016/j.plantsci.2020.110660>.
- Becht, E., McInnes, L., Healy, J., Dutertre, C.A., Kwok, I.W.H., Ng, L.G., Ginhoux, F., and Newell, E.W. (2018). Dimensionality reduction for visualizing single-cell data using UMAP. *Nat. Biotechnol.* **37**:38–44. <https://doi.org/10.1038/nbt.4314>.
- Bird, A.W., and Hyman, A.A. (2008). Building a spindle of the correct length in human cells requires the interaction between TPX2 and Aurora A. *J. Cell Biol.* **182**:289–300. <https://doi.org/10.1083/jcb.200802005>.
- Butler, A., Hoffman, P., Smibert, P., Papalexi, E., and Satija, R. (2018). Integrating single-cell transcriptomic data across different conditions, technologies, and species. *Nat. Biotechnol.* **36**:411–420. <https://doi.org/10.1038/nbt.4096>.
- Chen, C., Chen, H., Zhang, Y., Thomas, H.R., Frank, M.H., He, Y., and Xia, R. (2020). TBtools: an integrative toolkit developed for interactive analyses of big biological data. *Mol. Plant* **13**:1194–1202. <https://doi.org/10.1016/j.molp.2020.06.009>.
- Chen, E., Zhang, X., Yang, Z., Wang, X., Yang, Z., Zhang, C., Wu, Z., Kong, D., Liu, Z., Zhao, G., et al. (2017). Genome-wide analysis of the HD-ZIP IV transcription factor family in *Gossypium arboreum* and *GaHDG11* involved in osmotic tolerance in transgenic *Arabidopsis*. *Mol. Genet. Genom.* **292**:593–609. <https://doi.org/10.1007/s00438-017-1293-5>.
- Curaba, J., Herzog, M., and Vachon, G. (2003). *GeBP*, the first member of a new gene family in *Arabidopsis*, encodes a nuclear protein with DNA-binding activity and is regulated by *KNAT1*. *Plant J.* **33**:305–317. <https://doi.org/10.1046/j.1365-313x.2003.01622.x>.
- De Moura, S.M., Rossi, M.L., Artico, S., Grossi-de-Sa, M.F., Martinelli, A.P., and Alves-Ferreira, M. (2020). Characterization of floral morphoanatomy and identification of marker genes preferentially expressed during specific stages of cotton flower development. *Planta* **252**:71. <https://doi.org/10.1007/s00425-020-03477-0>.
- Deng, F., Tu, L., Tan, J., Li, Y., Nie, Y., and Zhang, X. (2012). *GbPDF1* is involved in cotton fiber initiation via the core cis-element HDZIP₂ATATHB₂. *Plant Physiol.* **158**:890–904. <https://doi.org/10.1104/pp.111.186742>.
- Gao, Y., Wang, H., Liu, C., Chu, H., Dai, D., Song, S., Yu, L., Han, L., Fu, Y., Tian, B., and Tang, L. (2018). De novo genome assembly of the red silk cotton tree (*Bombax ceiba*). *GigaScience* **7**:giy051. <https://doi.org/10.1093/gigascience/giy051>.
- Goldy, C., Pedroza-Garcia, J.A., Breakfield, N., Cools, T., Vena, R., Benfey, P.N., De Veylder, L., Palatnik, J., and Rodriguez, R.E. (2021). The *Arabidopsis* GRAS-type SCL28 transcription factor controls the mitotic cell cycle and division plane orientation. *Proc. Natl. Acad. Sci. USA* **118**, e2005256118. <https://doi.org/10.1073/pnas.2005256118>.
- Gray, J.E., Holroyd, G.H., van der Lee, F.M., Bahrami, A.R., Sijmons, P.C., Woodward, F.I., Schuch, W., and Hetherington, A.M. (2000). The *HIC* signalling pathway links CO₂ perception to stomatal development. *Nature* **408**:713–716. <https://doi.org/10.1038/35047071>.
- Guan, X.Y., Li, Q.J., Shan, C.M., Wang, S., Mao, Y.B., Wang, L.J., and Chen, X.Y. (2008). The HD-Zip IV gene *GaHOX1* from cotton is a functional homolog of the *Arabidopsis* *GLABRA2*. *Physiol. Plantarum* **134**:174–182. <https://doi.org/10.1111/j.1399-3054.2008.01115.x>.
- Haigler, C.H., Betancur, L., Stiff, M.R., and Tuttle, J.R. (2012). Cotton fiber: a powerful single-cell model for cell wall and cellulose research. *Front. Plant Sci.* **3**. <https://doi.org/10.3389/fpls.2012.00104>.
- Herrmann, A., Livanos, P., Zimmermann, S., Berendzen, K., Rohr, L., Lipka, E., and Müller, S. (2021). KINESIN-12E regulates metaphase spindle flux and helps control spindle size in *Arabidopsis*. *Plant Cell* **33**:27–43. <https://doi.org/10.1093/plcell/koaa003>.
- Hu, H., He, X., Tu, L., Zhu, L., Zhu, S., Ge, Z., and Zhang, X. (2016). GhJAZ2 negatively regulates cotton fiber initiation by interacting with the R2R3-MYB transcription factor GhMYB25-like. *Plant J.* **88**:921–935. <https://doi.org/10.1111/tpj.13273>.
- Huang, G., Huang, J.Q., Chen, X.Y., and Zhu, Y.X. (2021). Recent advances and future perspectives in cotton research. *Annu. Rev. Plant Biol.* **72**:437–462. <https://doi.org/10.1146/annurev-applant-080720-113241>.
- Humphries, J.A., Walker, A.R., Timmis, J.N., and Orford, S.J. (2005). Two WD-repeat genes from cotton are functional homologs of the

Special fiber initiation process in *B. ceiba*

- Arabidopsis thaliana* TRANSPARENT TESTA GLABRA1 (TTG1) gene. Plant Mol. Biol. **57**:67–81. <https://doi.org/10.1007/s11103-004-6768-1>.
- Hwang, B., Lee, J.H., and Bang, D. (2018). Single-cell RNA sequencing technologies and bioinformatics pipelines. Exp. Mol. Med. **50**:1–14. <https://doi.org/10.1038/s12276-018-0071-8>.
- Ishida, T., Kurata, T., Okada, K., and Wada, T. (2008). A genetic regulatory network in the development of trichomes and root hairs. Annu. Rev. Plant Biol. **59**:365–386. <https://doi.org/10.1146/annurev.arplant.59.032607.092949>.
- Jakoby, M.J., Falkenhan, D., Mader, M.T., Brininstool, G., Wischnitzki, E., Platz, N., Hudson, A., Hülskamp, M., Larkin, J., and Schnittger, A. (2008). Transcriptional profiling of mature *Arabidopsis* trichomes reveals that NOECK encodes the MIXTA-like transcriptional regulator MYB106. Plant Physiol. **148**:1583–1602. <https://doi.org/10.1104/pp.108.126979>.
- Kirik, V., Simon, M., Huelskamp, M., and Schiefelbein, J. (2004). The ENHANCER OF TRY AND CPC1 gene acts redundantly with TRIPTYCHON and CAPRICE in trichome and root hair cell patterning in *Arabidopsis*. Dev. Biol. **268**:506–513. <https://doi.org/10.1016/j.ydbio.2003.12.037>.
- Lai, L.B., Nadeau, J.A., Lucas, J., Lee, E.K., Nakagawa, T., Zhao, L., Geisler, M., and Sack, F.D. (2005). The *Arabidopsis* R2R3 MYB proteins FOUR LIPS and MYB88 restrict divisions late in the stomatal cell lineage. Plant Cell **17**:2754–2767. <https://doi.org/10.1105/tpc.105.034116>.
- Larkin, J.C., Oppenheimer, D.G., Lloyd, A.M., Paparozzi, E.T., and Marks, M.D. (1994). Roles of the GLABROUS1 and TRANSPARENT TESTA GLABRA genes in *Arabidopsis* trichome development. Plant Cell **6**:1065–1076. <https://doi.org/10.1105/tpc.6.8.1065>.
- Lee, J., Das, A., Yamaguchi, M., Hashimoto, J., Tsutsumi, N., Uchimiya, H., and Umeda, M. (2003). Cell cycle function of a rice B2-type cyclin interacting with a B-type cyclin-dependent kinase. Plant J. **34**:417–425. <https://doi.org/10.1046/j.1365-313x.2003.01736.x>.
- Liang, Y.K., Dubos, C., Dodd, I.C., Holroyd, G.H., Hetherington, A.M., and Campbell, M.M. (2005). AtMYB61, an R2R3-MYB transcription factor controlling stomatal aperture in *Arabidopsis thaliana*. Curr. Biol. **15**:1201–1206. <https://doi.org/10.1016/j.cub.2005.06.041>.
- Liu, B., Zhu, Y., and Zhang, T. (2015). The R3-MYB gene GhCPC negatively regulates cotton fiber elongation. PLoS One **10**:e0116272. <https://doi.org/10.1371/journal.pone.0116272>.
- Liu, H., Hu, D., Du, P., Wang, L., Liang, X., Li, H., Lu, Q., Li, S., Liu, H., Chen, X., et al. (2021). Single-cell RNA-seq describes the transcriptome landscape and identifies critical transcription factors in the leaf blade of the allotetraploid peanut (*Arachis hypogaea* L.). Plant Biotechnol. J. **19**:2261–2276. <https://doi.org/10.1111/pbi.13656>.
- Liu, Z., Zhou, Y., Guo, J., Li, J., Tian, Z., Zhu, Z., Wang, J., Wu, R., Zhang, B., Hu, Y., et al. (2020). Global dynamic molecular profiling of stomatal lineage cell development by single-cell RNA sequencing. Mol. Plant **13**:1178–1193. <https://doi.org/10.1016/j.molp.2020.06.010>.
- Machado, A., Wu, Y., Yang, Y., Llewellyn, D.J., and Dennis, E.S. (2009). The MYB transcription factor GhMYB25 regulates early fibre and trichome development. Plant J. **59**:52–62. <https://doi.org/10.1111/j.1365-313X.2009.03847.x>.
- Millar, A.A., Clemens, S., Zachgo, S., Giblin, E.M., Taylor, D.C., and Kunst, L. (1999). CUT1, an *Arabidopsis* gene required for cuticular wax biosynthesis and pollen fertility, encodes a very-long-chain fatty acid condensing enzyme. Plant Cell **11**:825–838. <https://doi.org/10.1105/tpc.11.5.825>.
- Mravec, J., Petrášek, J., Li, N., Boeren, S., Karlova, R., Kitakura, S., Pařezová, M., Naramoto, S., Nodzyński, T., Dhonukshe, P., et al. (2011). Cell plate restricted association of DRP1A and PIN proteins is required for cell polarity establishment in *Arabidopsis*. Curr. Biol. **21**:1055–1060. <https://doi.org/10.1016/j.cub.2011.05.018>.
- Qin, Y., Sun, M., Li, W., Xu, M., Shao, L., Liu, Y., Zhao, G., Liu, Z., Xu, Z., You, J., et al. (2022). Single-cell RNA-seq reveals fate determination control of an individual fibre cell initiation in cotton (*Gossypium hirsutum*). Plant Biotechnol. J. **20**:2372–2388. <https://doi.org/10.1111/pbi.13918>.
- Qiu, X., Mao, Q., Tang, Y., Wang, L., Chawla, R., Pliner, H.A., and Trapnell, C. (2017). Reversed graph embedding resolves complex single-cell trajectories. Nat. Methods **14**:979–982. <https://doi.org/10.1038/nmeth.4402>.
- Rijavec, T. (2008). Kapok in technical textiles. Tekstilec **51**:319–331.
- Risso, D., Ngai, J., Speed, T.P., and Dudoit, S. (2014). Normalization of RNA-seq data using factor analysis of control genes or samples. Nat. Biotechnol. **32**:896–902. <https://doi.org/10.1038/nbt.2931>.
- Romeiro Motta, M., Zhao, X., Pastuglia, M., Belcram, K., Roodbarkelari, F., Komaki, M., Harashima, H., Komaki, S., Kumar, M., Bulankova, P., et al. (2022). B1-type cyclins control microtubule organization during cell division in *Arabidopsis*. EMBO Rep. **23**:e53995. <https://doi.org/10.1525/embr.202153995>.
- Schnittger, A., Schöbinger, U., Stierhof, Y.D., and Hülskamp, M. (2002). Ectopic B-type cyclin expression induces mitotic cycles in endoreduplicating *Arabidopsis* trichomes. Curr. Biol. **12**:415–420. [https://doi.org/10.1016/s0960-9822\(02\)00693-0](https://doi.org/10.1016/s0960-9822(02)00693-0).
- Shaikhali, J., Davoine, C., Brännström, K., Rouhier, N., Bygdell, J., Björklund, S., and Wingsle, G. (2015). Biochemical and redox characterization of the mediator complex and its associated transcription factor GeBPL, a GLABROUS1 enhancer binding protein. Biochem. J. **468**:385–400. <https://doi.org/10.1042/bj20150132>.
- Shan, C.M., Shangguan, X.X., Zhao, B., Zhang, X.F., Chao, L.M., Yang, C.Q., Wang, L.J., Zhu, H.Y., Zeng, Y.D., Guo, W.Z., et al. (2014). Control of cotton fibre elongation by a homeodomain transcription factor GhHOX3. Nat. Commun. **5**:5519. <https://doi.org/10.1038/ncomms6519>.
- Shangguan, X.X., Yang, C.Q., Zhang, X.F., and Wang, L.J. (2016). Functional characterization of a basic helix-loop-helix (bHLH) transcription factor GhDEL65 from cotton (*Gossypium hirsutum*). Physiol. Plantarum **158**:200–212. <https://doi.org/10.1111/plp.12450>.
- Sharma, N., Kispotta, S., and Mazumder, P. (2020). Immunomodulatory and anticancer activity of *Bombax ceiba* Linn leaf extract. Asian Pac. J. Trop. Biomed. **10**:426–432. <https://doi.org/10.4103/2221-1691.290134>.
- Shi, Y.H., Zhu, S.W., Mao, X.Z., Feng, J.X., Qin, Y.M., Zhang, L., Cheng, J., Wei, L.P., Wang, Z.Y., and Zhu, Y.X. (2006). Transcriptome profiling, molecular biological, and physiological studies reveal a major role for ethylene in cotton fiber cell elongation. Plant Cell **18**:651–664. <https://doi.org/10.1105/tpc.105.040303>.
- Shimizu, R., Ji, J., Kelsey, E., Ohtsu, K., Schnable, P.S., and Scanlon, M.J. (2009). Tissue specificity and evolution of meristematic WOX3 function. Plant Physiol. **149**:841–850. <https://doi.org/10.1104/pp.108.130765>.
- Skirycz, A., Radziejwoski, A., Busch, W., Hannah, M.A., Czeszejko, J., Kwaśniewski, M., Zanor, M.I., Lohmann, J.U., De Veylder, L., Witt, I., and Mueller-Roeber, B. (2008). The DOF transcription factor OBP1 is involved in cell cycle regulation in *Arabidopsis thaliana*. Plant J. **56**:779–792. <https://doi.org/10.1111/j.1365-313X.2008.03641.x>.
- Smertenko, A.P., Chang, H.Y., Sonobe, S., Fenyk, S.I., Weingartner, M., Bögrie, L., and Hussey, P.J. (2006). Control of the AtMAP65-1 interaction with microtubules through the cell cycle. J. Cell Sci. **119**:3227–3237. <https://doi.org/10.1242/jcs.03051>.
- Stewart, J.McD. (1975). Fiber initiation on the cotton ovule (*Gossypium hirsutum*). Am. J. Bot. **62**:723–730. <https://doi.org/10.2307/2442061>.

Plant Communications

Plant Communications

- Sunmonu, O.K., and Abdullahi, D.** (1992). Characterization of fibres from the plant *ceiba Pentandra*. *J. Textil. Inst.* **83**:273–274. <https://doi.org/10.1080/00405009208631197>.
- Tang, F., Lao, K., and Surani, M.A.** (2011). Development and applications of single-cell transcriptome analysis. *Nat. Methods* **8**:S6–S11. <https://doi.org/10.1038/nmeth.1557>.
- Tian, Y., Du, J., Wu, H., Guan, X., Chen, W., Hu, Y., Fang, L., Ding, L., Li, M., Yang, D., et al.** (2020). The transcription factor MML4_D12 regulates fiber development through interplay with the WD40-repeat protein WDR in cotton. *J. Exp. Bot.* **71**:3499–3511. <https://doi.org/10.1093/jxb/eraa104>.
- Trapnell, C., Cacchiarelli, D., Grimsby, J., Pokharel, P., Li, S., Morse, M., Lennon, N.J., Livak, K.J., Mikkelsen, T.S., and Rinn, J.L.** (2014). The dynamics and regulators of cell fate decisions are revealed by pseudotemporal ordering of single cells. *Nat. Biotechnol.* **32**:381–386. <https://doi.org/10.1038/nbt.2859>.
- Ueguchi-Tanaka, M., Hirano, K., Hasegawa, Y., Kitano, H., and Matsuoka, M.** (2008). Release of the repressive activity of rice DELLA protein SLR1 by gibberellin does not require SLR1 degradation in the *gid2* mutant. *Plant Cell* **20**:2437–2446. <https://doi.org/10.1105/tpc.108.061648>.
- Wagner, A., Regev, A., and Yosef, N.** (2016). Revealing the vectors of cellular identity with single-cell genomics. *Nat. Biotechnol.* **34**:1145–1160. <https://doi.org/10.1038/nbt.3711>.
- Walford, S.A., Wu, Y., Llewellyn, D.J., and Dennis, E.S.** (2011). GhMYB25-like: a key factor in early cotton fibre development. *Plant J.* **65**:785–797. <https://doi.org/10.1111/j.1365-313X.2010.04464.x>.
- Walford, S.A., Wu, Y., Llewellyn, D.J., and Dennis, E.S.** (2012). Epidermal cell differentiation in cotton mediated by the homeodomain leucine zipper gene, *GhHD-1*. *Plant J.* **71**:464–478. <https://doi.org/10.1111/j.1365-313X.2012.05003.x>.
- Wang, G., Zhao, G.H., Jia, Y.H., and Du, X.M.** (2013). Identification and characterization of cotton genes involved in fuzz-fiber development. *J. Integr. Plant Biol.* **55**:619–630. <https://doi.org/10.1111/jipb.12072>.
- Wang, M., Tu, L., Yuan, D., Zhu, D., Shen, C., Li, J., Liu, F., Pei, L., Wang, P., Zhao, G., et al.** (2019). Reference genome sequences of two cultivated allotetraploid cottons, *Gossypium hirsutum* and *Gossypium barbadense*. *Nat. Genet.* **51**:224–229. <https://doi.org/10.1038/s41588-018-0282-x>.
- Special fiber initiation process in *B. ceiba***
- Wang, S., Wang, J.W., Yu, N., Li, C.H., Luo, B., Gou, J.Y., Wang, L.J., and Chen, X.Y.** (2004). Control of plant trichome development by a cotton fiber MYB gene. *Plant Cell* **16**:2323–2334. <https://doi.org/10.1105/tpc.104.024844>.
- Yang, C., and Ye, Z.** (2013). Trichomes as models for studying plant cell differentiation. *Cell. Mol. Life Sci.* **70**:1937–1948. <https://doi.org/10.1007/s00018-012-1147-6>.
- Yang, K., Wang, H., Xue, S., Qu, X., Zou, J., and Le, J.** (2014). Requirement for A-type cyclin-dependent kinase and cyclins for the terminal division in the stomatal lineage of *Arabidopsis*. *J. Exp. Bot.* **65**:2449–2461. <https://doi.org/10.1093/jxb/eru139>.
- Zeng, J., Zhang, M., Hou, L., Bai, W., Yan, X., Hou, N., Wang, H., Huang, J., Zhao, J., and Pei, Y.** (2019). Cytokinin inhibits cotton fiber initiation by disrupting PIN3a-mediated asymmetric accumulation of auxin in the ovule epidermis. *J. Exp. Bot.* **70**:3139–3151. <https://doi.org/10.1093/jxb/erz162>.
- Zhang, M., Zeng, J.Y., Long, H., Xiao, Y.H., Yan, X.Y., and Pei, Y.** (2017). Auxin regulates cotton fiber initiation via GhPIN-mediated auxin transport. *Plant Cell Physiol.* **58**:385–397. <https://doi.org/10.1093/pcp/pcw203>.
- Zhang, T.Q., Chen, Y., Liu, Y., Lin, W.H., and Wang, J.W.** (2021). Single-cell transcriptome atlas and chromatin accessibility landscape reveal differentiation trajectories in the rice root. *Nat. Commun.* **12**:2053. <https://doi.org/10.1038/s41467-021-22352-4>.
- Zhang, T.Q., Xu, Z.G., Shang, G.D., and Wang, J.W.** (2019). A single-cell RNA sequencing profiles the developmental landscape of *Arabidopsis* root. *Mol. Plant* **12**:648–660. <https://doi.org/10.1016/j.molp.2019.04.004>.
- Zhou, Y., Zhang, Z.T., Li, M., Wei, X.Z., Li, X.J., Li, B.Y., and Li, X.B.** (2015). Cotton (*Gossypium hirsutum*) 14-3-3 proteins participate in regulation of fibre initiation and elongation by modulating brassinosteroid signalling. *Plant Biotechnol. J.* **13**:269–280. <https://doi.org/10.1111/pbi.12275>.
- Ziegenhain, C., Vieth, B., Parekh, S., Reinius, B., Guillaumet-Adkins, A., Smets, M., Leonhardt, H., Heyn, H., Hellmann, I., and Enard, W.** (2017). Comparative analysis of single-cell rna sequencing methods. *Mol. Cell* **65**:631–643.e4. <https://doi.org/10.1016/j.molcel.2017.01.023>.